Pergamon

Int. J. Heat Mass Transfer. Vol. 38, No. 13, pp. 2383–2393, 1995

0017-9310/95 $9.50+0.00

0017-9310(94)00362-9

An experimental investigation of the solidification process in a V-shaped sump

R. BURTON, G. YANG, Z. F. DONG and M. A. EBADIAN†
Department of Mechanical Engineering, Florida International University, Miami, FL 33199, U.S.A.

(*Received* 11 *April* 1994 *and in final form* 28 *November* 1994)

Abstract—An experimental study of binary mixture solidification in a V-shaped sump is conducted. NH_4Cl–H_2O is used as the phase change material. The variations of temperature, concentration, as well as the location of the interface front, are measured and reported in this investigation. The results indicate that the solidification process exhibits totally different behavior when the initial component of the solution is varied. For a hypoeutectic solution, the columnar solidification in the dendritic interface is the dominant mechanism. For the hypereutectic solution, both columnar and equiaxed solidification are important. The solidification starts as the equiaxed dendrites grow and coalesce in the entire solution. They then descend and settle at the bottom of the sump to form a loose, mushy zone. The solid region grows underneath the mushy zone.

1. INTRODUCTION

Solidification is a phase transformation process that is accompanied by the release of thermal energy. The common feature of a system undergoing solid–liquid phase change is the existence of a moving boundary that separates the two phases of the solution with different thermophysical properties. The majority of commercial metal products are composed of alloys of two or more constituent elements, making them differ in many respects from the solid structure of a pure substance [1, 2]. During the solidification of binary mixtures, the density of the liquid varies with both temperature and concentration. Thus, natural convection can be caused by both thermally and solutally induced density gradients. Previous researchers indicate that the major cause of structural defects and inhomogeneity (macrosegration and microsegration) during solidification is attributed to an improper convection flow pattern in the melt sump and the mushy zone [1]. Therefore, knowledge of the transport phenomena of double diffusive convection in the melt sump is essential for maintaining satisfactory control over the casting process. Due to the complexity of double diffusive convection during the solidification process, theoretical study on this topic is still in the developing stage [3] and experimental study is still the most powerful means for understanding this basic phenomenon. Many experimental studies on this topic have been conducted using different kinds of solutions. Liquid metals have been applied to study the solidification process by some researchers (Al–Cu alloy) [4] and (Pb–Sn alloy) [5]. Since the liquid metal is opaque, it is very difficult to determine the flow pattern and the moving solid front interface during the experiment. Therefore, transparent solutions are usually applied to analogue alloy solidification. The NH_4Cl–H_2O solution was used to measure both velocity and temperature distributions in the solution [6, 7], and a solidification test was conducted by using an Na_2CO_3–H_2O solution [8, 9]. Recently, the solidification process in a rectangular cavity was also studied by using the NH_4Cl–H_2O system [10, 11]. The above mentioned survey of the literature indicates that the majority of existing experimental results were obtained from the rectangular cross section test sump, which focused only on static ingot solidification. During the continuous casting process, melted material is poured into a water-cooled mold and exits the mold from the bottom. After heat is lost to the mold wall, the material nearest the cooled mold is solidified first to form a crust with the liquid material in the center. This crust is continuously withdrawn from the bottom. The material in the center usually needs additional time to solidify, which results in a V-shaped liquid sump. The angle of the V-shape is about 4–16°, which usually depends on the crust movement velocity and the thermal properties of the casting material. What is the effect of the oblique walls of the V-shaped boundary on the solidification process of the binary solution? The surveys indicate that no such information is available in the open literature. As a first step for studying the V-shaped solidification process in continuous casting, this paper presents the primary experimental results of temperature, concentration, and the moving solid front interface during the solidification process in a fixed V-shaped sump.

2. TEST FACILITY AND INSTRUMENTATION

A test facility, which includes a test sump and cooling system, was constructed to model the two-dimen-

† Author to whom correspondence should be addressed.

NOMENCLATURE

C	concentration	Subscripts	
T	temperature	c	cooling
t	time	e	eutectic
x	vertical location	o	initial.
y	horizontal location.		

sional solidification process in a V-shaped sump. Figure 1 is a schematic of the V-shaped test sump. The test sump consists of two aluminum side walls, front and back glass windows, and a top cover. The dimensions of the test sump are 28 cm × 8 cm × 29 cm (length × width × height), respectively. The galleries, which were 8 mm wide × 12 mm deep, were machined into the back surfaces of the aluminum side walls to serve as a channel for the coolant. Five J-type thermocouples were installed inside each side wall to measure the wall temperature. Four triangular glass plates were mounted between the two side walls to divide the test sump into three chambers. A rectangular glass plate cover was placed at the top of the sump to ensure that these three chambers were airtight. In order to prevent vapor condensation on the front and rear windows, the front and rear chambers (1.5 cm length on each side) were kept in a vacuum during the test. The middle chamber of the test sump is 25 cm in length, which was filled with the NH_4Cl–H_2O solution, and was also kept in a vacuum during the test to extract the gas from the solution. The test sump was covered by a syphon box to insulate it from the ambient.

Figure 2 shows the cooling system and the instruments used in this investigation. The cooling system includes three refrigerators and the associated control valves and piping. Two 425 watt Model N01268 digital refrigerated circulator baths (Refrigerators I and II) were applied to keep the side walls at a desired temperature during a normal test. A 175 W Model N01267 digital refrigerated circulator bath (Refrigerator III) was used to set the initial temperature.

Seventeen thermocouples were installed to monitor the temperature distribution of the solution. These thermocouples were mounted on a plexiglas frame to ensure that they remained in place during the solidification process. The thermocouples were arranged in four horizontal lines, with the top line located 1 cm below the solution. The locations of each thermocouple are listed in detail in Table 1, where the origin points ($x = 0$ and $y = 0$) are defined at the bottom corner of the test chamber, as seen in Fig. 2. All thermocouples were calibrated individually after they were installed. The thermocouples were connected to an HP data acquisition system (Model No. 3852A) and monitored by a personal computer. The uncertainty of the temperature measurement is ± 0.3°C. The uncertainty of the thermocouple location is less than ± 1 mm.

Aqueous ammonium chloride (NH_4Cl–H_2O) was chosen as the test solution due to its similar solidification behavior as the liquid metal, and for its semi-

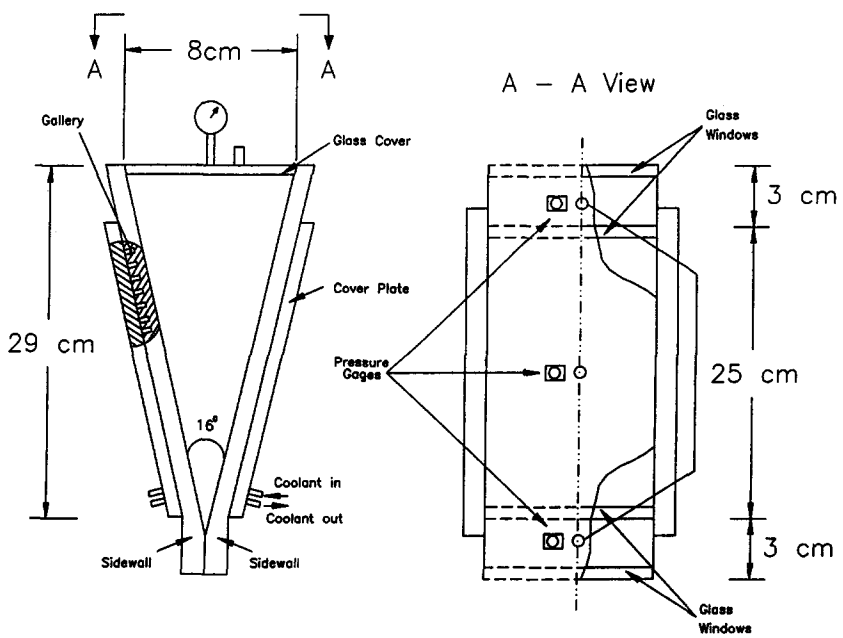

Fig. 1. Schematic representation of the test section.

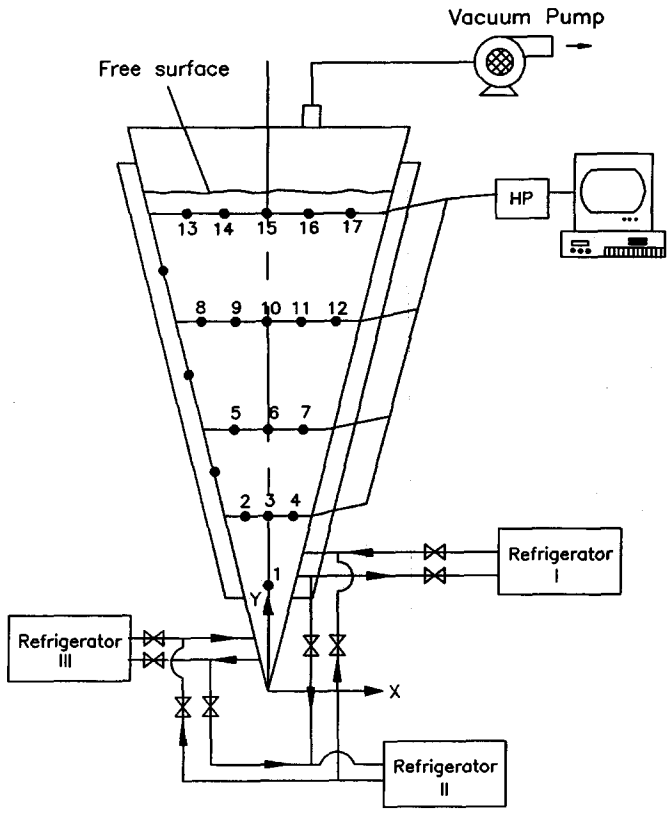

Fig. 2. Schematic representation of the cooling system.

Table 1. Location of the thermocouples

Number of thermocouples	x [cm]	y [cm]
1	0	1.52
2	−1.02	6.60
3	0	6.60
4	1.52	6.60
5	−1.27	12.7
6	0	12.7
7	1.78	12.7
8	−1.78	17.27
9	−0.76	17.27
10	0	17.27
11	1.27	17.27
12	2.29	17.27
13	−2.54	22.35
14	−1.02	22.35
15	−0.51	22.35
16	1.03	22.35
17	2.81	22.35

transparency. The eutectic temperature and composition of the NH_4Cl–H_2O are $T_e = -15.4°C$ and $C_e = 19.7\%$, respectively. The concentration measurement was conducted by extracting the solution through a set of syringes (test probes). Nine syringes were used to measure the liquid concentration. During solidification, the tips of these syringes were located in different x and y positions. However, 30 min after the start of the test the majority of the locations of the tips of the syringes were either occupied by ice or were mushy. Only two syringes (probes C and F) could provide us with information during the entire process. Both probes C and F were located along the centerline of the sump, with the tips located at 4 cm and 6.89 cm below the surface of the liquid (or 23 cm and 20.11 cm from the bottom corner). An ABBE 2WAJ refractometer was used to measure the refractive index of the extracted solution. The refractive index was then transferred to the concentration through a chart, which was created by measuring a set of known concentrations. Uncertainty in the placement of the probe was about ± 1 mm. Since only a very small amount of liquid was extracted during the test, the effect of the concentration gradient near the probe tip was minor. The estimated uncertainty of the concentration measurement was about $\pm 0.5\%$.

A video camera was used to capture the movement of the solid–liquid fronts during the test. The video tapes were then processed by an image processing package (DATA Translation DT 2855) to determine the location of the solid–mushy–liquid fronts and to calculate the solidification rate. Basically, the test chamber is long enough to be considered a two-dimensional chamber (2D). Since the solid–mushy–liquid fronts produced different light reflections, the image captured by the video camera could easily distinguish these three zones. Figure 3 shows the three images at hypoeutectic, eutectic and hypereutectic conditions. The light areas in the pictures indicate the mushy

Fig. 3. Video image of the interface front.

Table 2. Summary of the experimental conditions

Test run	C_o [%]	T_o [°C]	T_c [°C]
1	19.7	5	−20
2	5.0	5	−10
3	15.0	5	−15
4	25	15	−20

(dendritic) zones. It is worthwhile to point out that in the eutectic condition ($C_o = 19.7\%$), the bright lines represent the liquid–solid interface.

3. EXPERIMENTAL PROCEDURE

During the solidification process, the gas originally absorbed in the solution was released. These air bubbles can drive the surrounding liquid to form an upward flow. In order to make the solution free from gas when a new solution was poured into the test chamber, the solution was solidified and melted at least three times. The test chamber was also kept in a vacuum to prevent the solution from reabsorbing the gas. The results of four test runs were selected and are presented in this paper. Each test was repeated four to five times. Table 2 provides the information regarding the initial temperature, concentration, and the cooling temperature in each test run. Test Run 1 represents the case of the eutectic solidification process. Test Runs 2 and 3 indicate the case of hypoeutectic solidification, while Test Run 4 is hypereutectic solidification.

The first step of the test was to set up a uniform initial temperature, T_o, for the test solution. Refrigerator III was connected to the cooling line to provide a desired temperature through the two side walls. Thermocouples were closely monitored to check the temperature of the solution. The maximum temperature difference inside the solution was less than 0.5°C before starting the experiment. During the time to set up the initial temperature, Refrigerators I and II were disconnected from the cooling line and run to establish the required cooling temperature, T_c. After thermal uniformity was reached in the solution, Refrigerators I and II were connected to the cooling line and Refrigerator III was disconnected, after which the experiment began.

During the test, the temperature was continuously monitored at every 1 min interval for the first hour and at 5 min intervals after that. The video camera continuously recorded so that the tapes could be viewed later. The concentration measurements were conducted every 30 min. Although the test rack initially included nine test probes (syringes), due to solidification, only two probes could provide the concentration information throughout the test. The test times for each run were significantly different depending on the initial concentration, which varied from 2 to 8 h.

4. RESULTS AND DISCUSSION

The simplest case of solidification of a binary mixture is the case of eutectic composition. In eutectic composition, the solution exhibits the phase change behavior of a pure substance, and the convective flow is driven solely by the thermal buoyancy force. Figure 4 shows the history of the solid–liquid interfaces in Test Run 1. A half-hour after starting, Fig. 4(a) shows that the solid interface appeared on the side walls. The

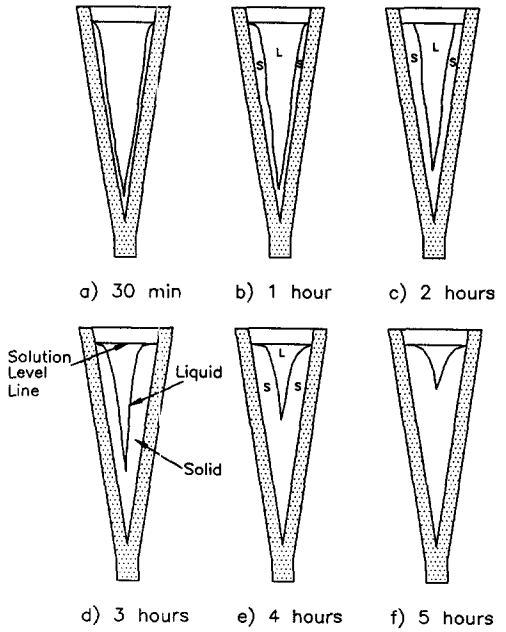

Fig. 4. Interface front in the $C_0 = 19.7\%$ solution.

solid–liquid interfaces appeared very smooth and were well distributed along both surfaces. Since the solution temperature in the center of the test chamber was higher than that near the interface, a thermally driven natural convection was generated. The fluid near the cooling interface flowed down and then moved up in the center region to form two recirculation loops. As time elapsed, however, the solidified region increased, and the liquid region always remained in a V-shape, as seen in Fig. 4(b)–(f).

For the solution with a hypoeutectic composition, the solute will be ejected during the solidification process and the two-phase interface is characterized as the mushy zone. As a result, there exists a high concentration region in and near the interdendritic zone. Since the solute was denser than the solution, a downward flow was generated along the interface by the solute driven natural convection, which was in the same direction as that of the thermal by driven convection. Figures 5 and 6 show the variation of the temperature contours during the solidification process in a hypoeutectic composition solution (Test Run 2). In this test, a 5% NH_4Cl composition solution was used with initial and cooling temperatures of $T_0 = 5°C$ and $T_c = -10°C$, respectively. Figure 5 shows the temperature variation of thermocouples, Nos 8, 9 and 10. These three thermocouples are located about 6.8 cm below the solution surface, where thermocouple No. 8 is 2 mm away from the side wall, and thermocouple No. 10 is in the center chamber. This figure indicates that the readings of thermocouples Nos 9 and 10 were closer to each other, and that of No. 8 was always far below that of the other two. It is also interesting to note that instead of continuously reducing the temperature in locations Nos 9 and 10, the reading of No. 8 displayed a sudden increase in the early stage. In the first 20 min, the solution temperature near the side walls (No. 8) steadily dropped to $-5.6°C$, which is lower than the freezing temperature for this concentration. This overcooling endured a few minutes until the first dendrites appeared. Visual observation indicated that the dendritic region spread very fast to cover the entire side wall surfaces in less than 1 min, while at the same time, the thermocouple reading of No. 8 jumped to $-2.8°C$. Figure 6 shows the temperature variation

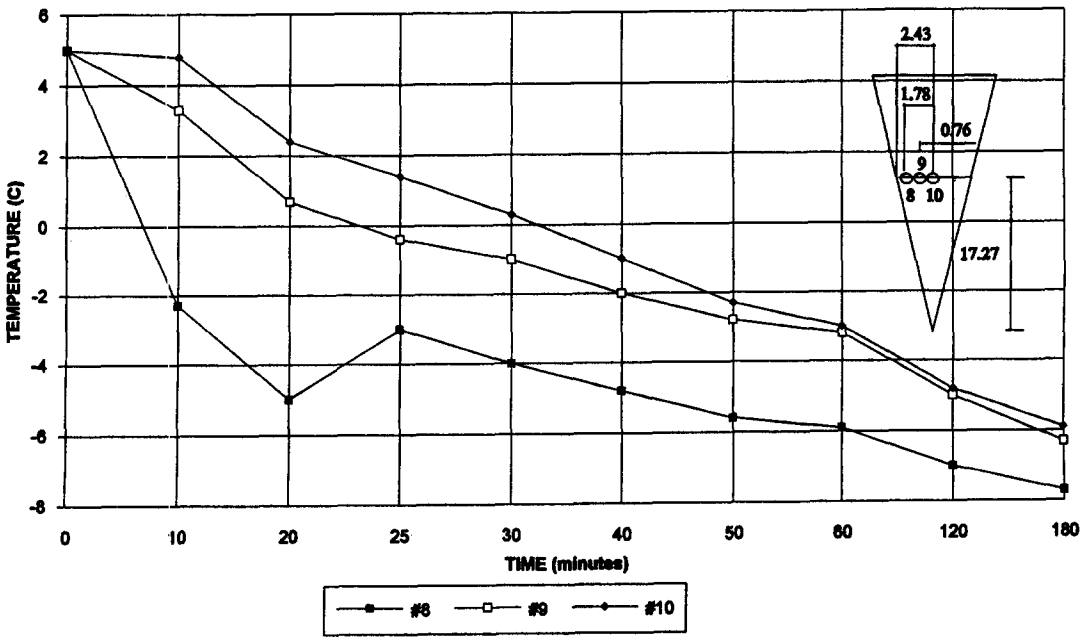

Fig. 5. Temperature history for the horizontal thermocouples ($C_0 = 5\%$, $T_c = -10°C$, $T_i = 5°C$).

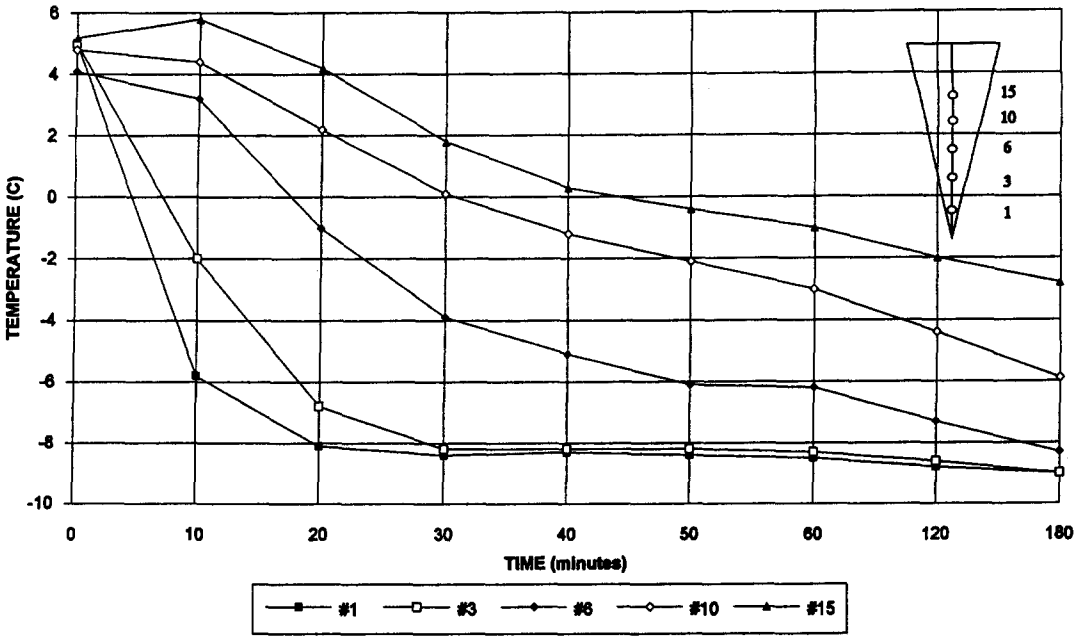

Fig. 6. Temperature history for the vertical thermocouples ($C_o = 5\%$, $T_c = -10°C$, $T_i = 5°C$).

along the centerline of the test chamber. The vertical locations of thermocouples, Nos 1, 3, 6, 10 and 15, are 22.5, 17.4, 11.3, 6.8 and 1.7 cm, respectively. This figure indicates that temperatures in all five locations steadily dropped as time elapsed, and the temperature in the upper point was always higher than that in the lower point. Figure 7 shows the movement of the solid–liquid interface fronts. At $t = 30$ min, Fig. 7(a), visual observation indicated that the solidified region was composed of mainly long and coarse dendrite interfaces. As time elapsed, the dendrite became shorter and finer, and the solid region appeared, Fig. 7(b). Since the solute-rich fluid continuously flowed down along the interface region, the concentration in the bottom region of the test chamber steadily increased, which delayed the solidifying process in this region. Figures 7(c) and (d) show that the interface fronts moved close to each other, and left a long narrow gap between them. Figure 8 shows that the concentration changed with time in this case. The probes, C and F, are located below the solution surface. The figure indicates that the concentration increased as time elapsed. After 90 min, the concentration at point C almost reached 10%.

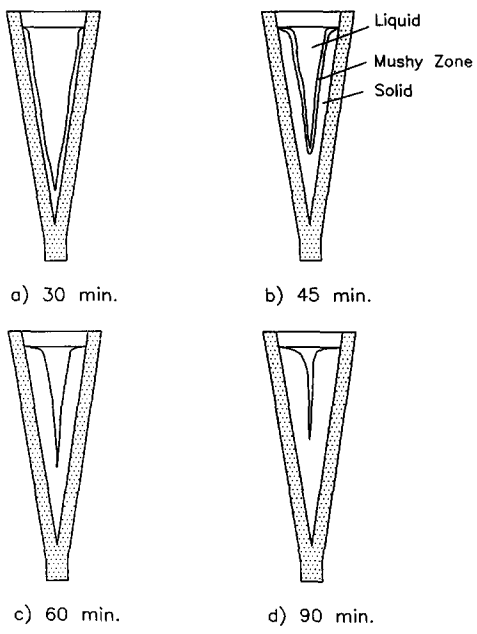

Fig. 7. Interface front in the $C_o = 5\%$ solution.

Figure 9 shows another case of solidification in a hypoeutectic composition of 15% (Test Run 3). The dendrites appeared 15 min after the test. Columnar dendrites occurred on the walls of the top half of the chamber. Some of the loose columnar dendrites fell while joined with the equiaxed dendrites to pack at the bottom corner, forming a mushy zone. Figure 9(a) illustrates the interfaces of the liquid–mushy–solid front at $t = 30$ min. It can be seen that a very thin solid built up along the wall, with a thick layer of the mushy zone between the solid and the solution. Both the mushy and solid regions increased after that, as seen in Fig. 6 ($t = 60$ min.). After one hour, the interface between the mushy zone and the solution changed slowly, unlike the solid region's rapid increase (Fig. 9(c) and (d)). At $t = 3$ h, the mushy zone near the bottom corner became solid and at $t = 4.5$ h, the mushy zone almost disappeared. Figure 10 indicates that the concentration at points C and F continuously increased until reaching eutectic concentration, around $t = 3$ h, then remained constant, which can explain why the mushy zone disappeared later on.

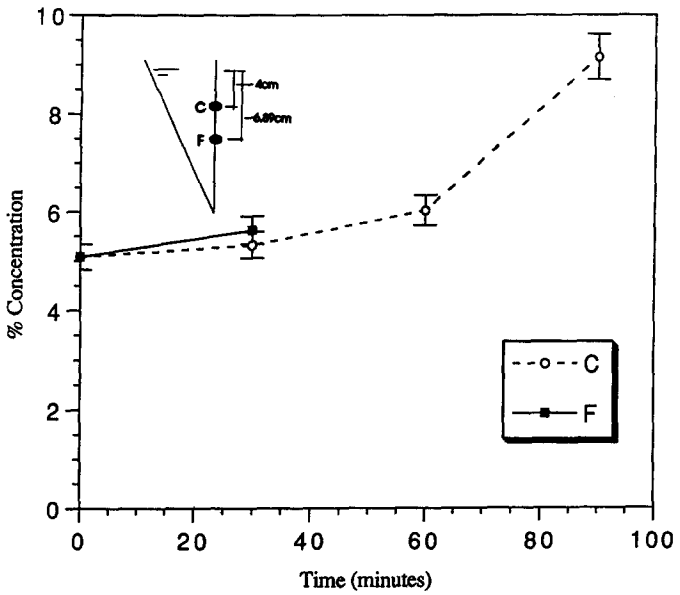

Fig. 8. Concentration variation in the $C_o = 5\%$ solution.

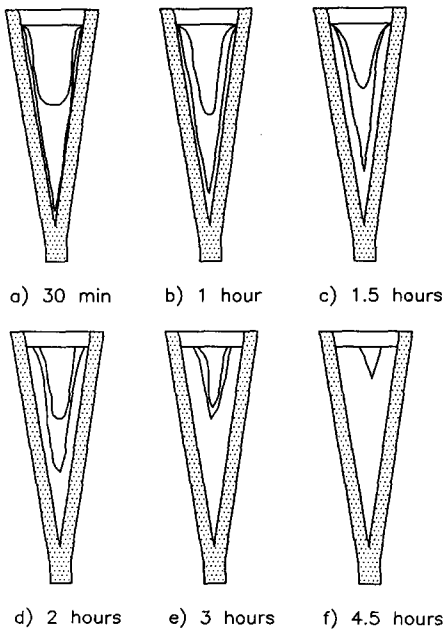

Fig. 9. Interface front in the $C_o = 15\%$ solution.

Figure 11 shows the temperature history for thermocouples Nos 8, 9 and 10. This figure indicates that the horizontal temperature in this case was much more uniform than in the case of the 5% composition (Fig. 5). Also, no overcooling phenomenon was observed in this case. Figure 12 shows the vertical temperature distributions along the centerline. This figure indicates that the temperature in the upper point was always higher than that in the lower point, which is consistent with the result for the case of the 5% composition.

In contrast to the hypoeutectic composition, the ejection of water-rich interdendritic fluid will induce an upward flow in the hypereutectic composition solution, which is opposite to the thermally driven flow. Therefore, totally different solidification behavior can be expected in these two cases. Figure 13 shows that the interface front moved with time in a hypoeutectic component solution, where the initial component is 25%, $T_i = 15°C$, and $T_c = -20°C$. Visual observation indicated that a few minutes after starting the test, the equiaxed dendrites appeared at the bottom corner first, and then in the entire domain. Many tiny solid particles grew and coalesced as they descended. After about another 5 min, the dendrites settled down to form a mushy zone at the bottom, as seen in Fig. 13(a). The mushy zone increased slowly after that, and the solid zone grew under the mushy zone, as seen in Fig. 13(b)–(d). At $t = 1$ h, no solid zone could be seen at the top of the sump. The solid zone appeared at the top of the sump at $t = 2$ h, and the surface of the solid zone was almost smooth. The solid region continued to grow and the loose mushy zone was reduced. The interface of the solution and the solid at the top of the sump remained smooth. Figure 14 shows that the concentration at points C and F reached a eutectic value after around 2 h and remained that way. The results of the horizontal temperature measurements are presented in Fig. 15. This figure indicates that the temperature near the wall at thermocouple No. 8 was much lower than the inside solutions (Nos 9 and 10) in the first 2 h. However, the temperature difference between thermocouples Nos 9 and 10 was very minor. It is interesting to see the difference between Figs. 15 and 5, or 11. Instead of a smooth variation of the temperature, Fig. 15 shows the fluctuation of the temperature with time. This represents the existence of equiaxed solidification. Figure 16 shows the temperature distribution along the vertical direction. Like that in Fig. 15, the temperature fluctuated with time before the solution near this point

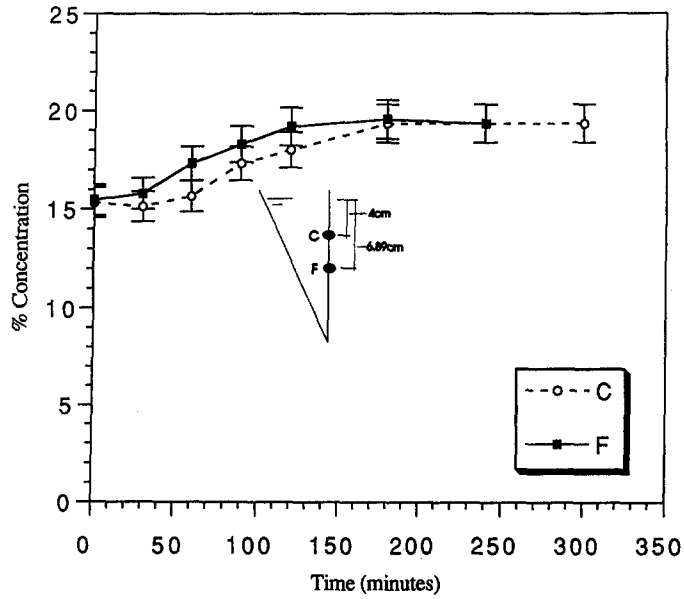

Fig. 10. Concentration variation in the $C_o = 15\%$ solution.

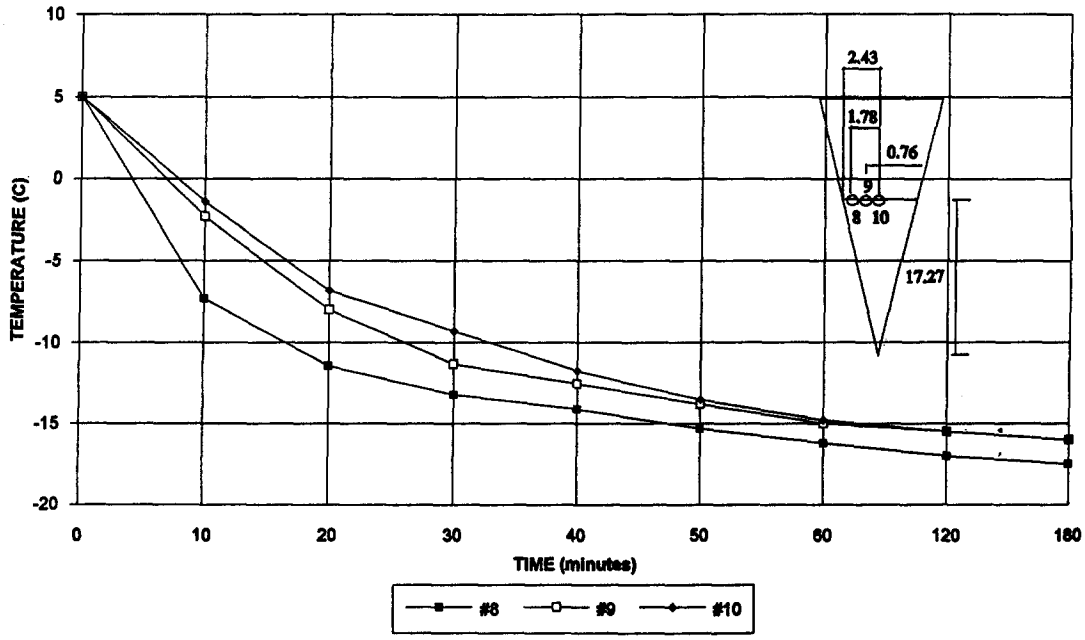

Fig. 11. Temperature history for the horizontal thermocouples ($C_o = 15\%$, $T_c = -15°C$, $T_i = 0°C$).

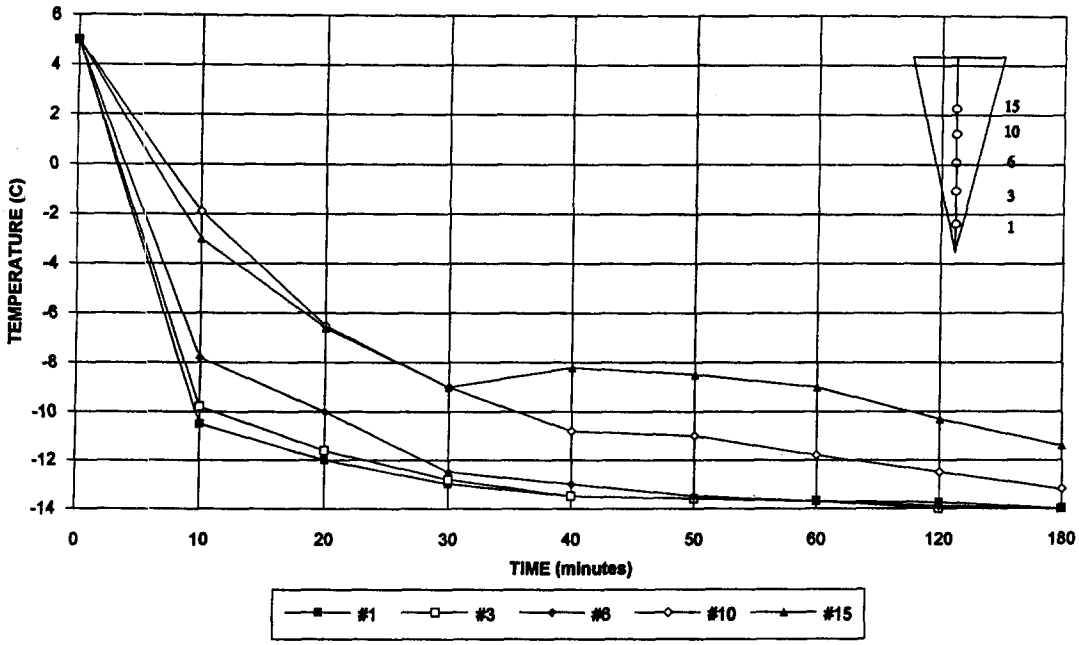

Fig. 12. Temperature history for the vertical thermocouples ($C_o = 15\%$, $T_c = -15°C$, $T_i = 0°C$).

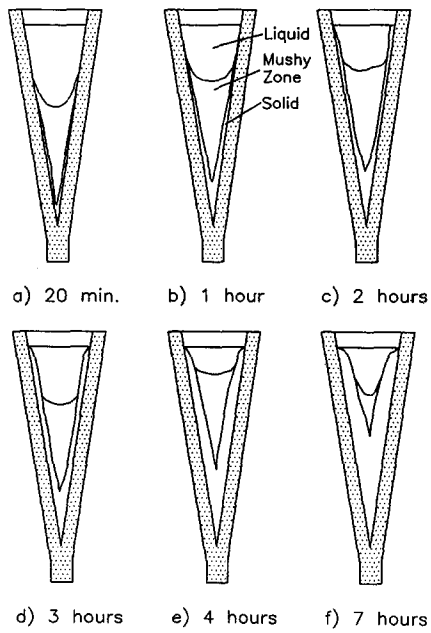

Fig. 13. Interface front in the $C_o = 25\%$ solution.

solidified. It can be seen that the temperature in thermocouple No. 10 was higher than that in thermocouple No. 15, between 10 and 120 min. That is, the temperature near the top free surface was lower than that in the liquid center. This temperature distribution reflects the effect of the solute-driven flow. As the water-rich fluid was ejected from the dendritic interface, it flowed upward along the interface and then recirculated through the top free surface region. It is interesting to compare the temperature change behaviors of Figs. 15 and 16 and that of Figs. 5, 6, 11 and 12. In Figs. 15 and 16, the temperatures at all points fell below 5°C in the first few minutes. The equilibrium phase diagram for NH_4Cl–H_2O [10] indicates that this temperature was below the phase change temperature in the 25% concentration solution, which is why the equiaxed dendrites appeared in the entire solution. In the 5% and 15% initial concentration solutions, a considerable temperature difference existed, which is why the dendrites and the solidification mainly occurred on the side walls.

5. SUMMARY

An experimental study of the solidification for a binary mixture in a V-shaped test chamber has been conducted. Aqueous ammonium chloride was chosen as the phase change material. The effects of the NH_4Cl concentration on solidification have been examined by changing the initial component of the solution. In the eutectic solution, the solidification characterized as a smooth discrete interface always maintained a V-shaped configuration. In the hypoeutectic solution, the solidification mainly depended on the columnar growth on the dendritic interface. However, depending on the initial concentration, the shape of the final

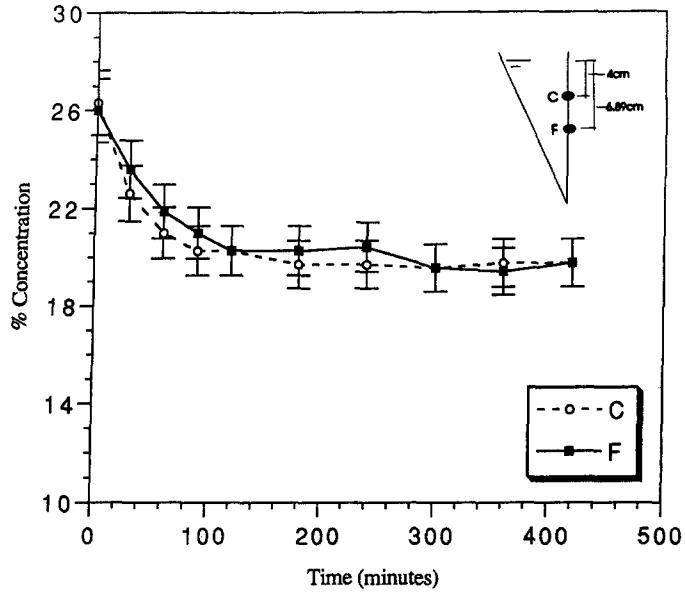

Fig. 14. Concentration variation in the $C_o = 25\%$ solution.

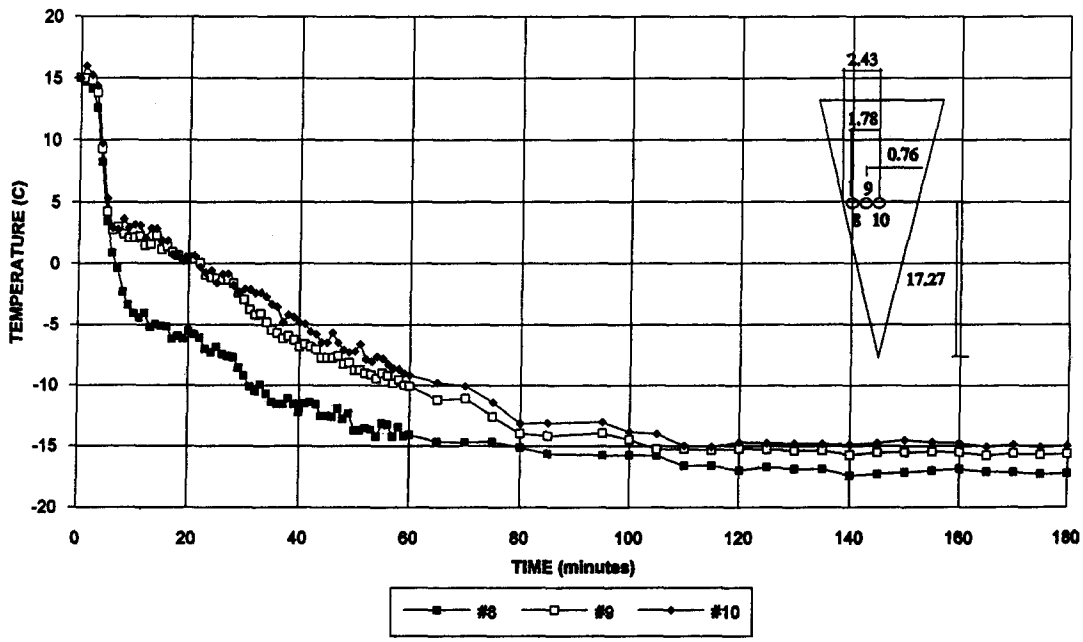

Fig. 15. Temperature history for the horizontal thermocouples ($C_o = 25\%$, $T_c = -20°C$, $T_i = 15°C$).

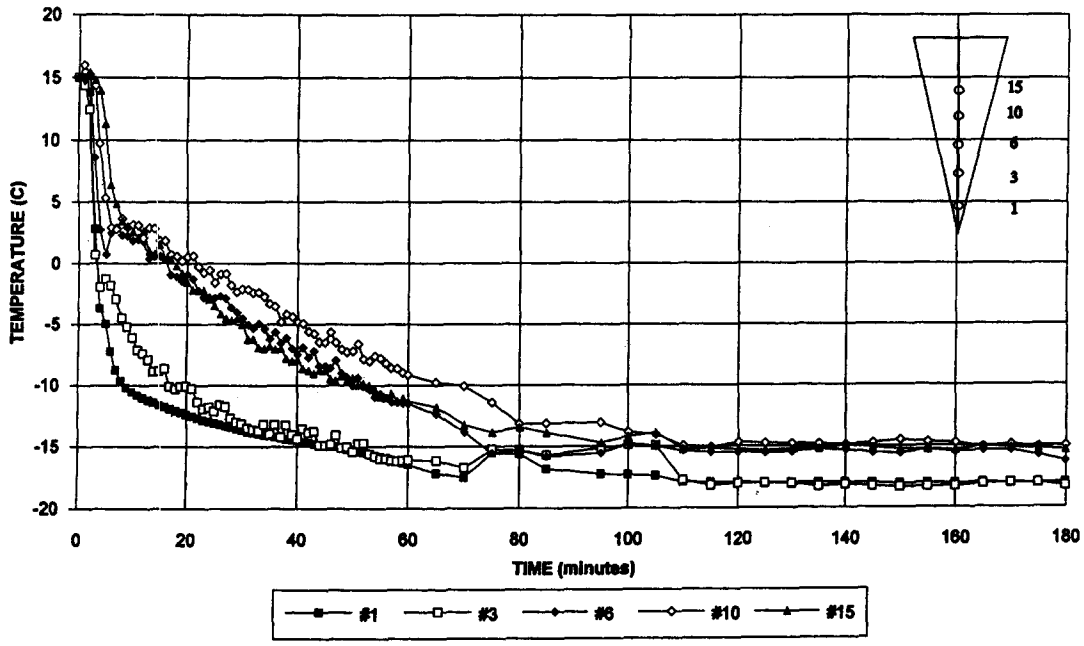

Fig. 16. Temperature history for the vertical thermocouples ($C_0 = 25\%$, $T_c = -20°C$, $T_i = 15°C$).

liquid–solid interface may differ totally, which may significantly affect the quality of the final product. In the hypereutectic solution, equiaxed solidification is important. In the beginning, the equiaxed dendrites appeared in the entire solution and then grew and coalesced as they descended and formed a loose mushy zone. The solid region then grew under the mushy zone.

Acknowledgements—The results presented in this paper were obtained in the course of research sponsored by the National Science Foundation. The authors would also like to thank Mr G. Martin, F. Desir and G. Hoo for their assistance throughout this study.

REFERENCES

1. K. M. Fisher, The effects of fluid flow on the solidification of industrial castings and ingots, *Physico-Chem. Hydrodyn.* **2,** 311–326 (1981).
2. R. Viskanta, Natural convection in melting and solidification. In *Natural Convection* (Edited by S. Kakac, W. Aung and R. Viskanta), p. 845. Hemisphere, New York (1985).
3. F. P. Incropera and R. Viskanta, Effect of convection on the solidification of binary mixtures. In *Heat and Mass Transfer in Materials Process* (Edited by I. Tanasawa and N. Lior), p. 295. Hemisphere, New York (1992).
4. R. Mehrabian, M. A. Keane and M. C. Flemings, Experiments on macrosegregation and freckle formation, *Met. Trans.* **1,** 3238–3241 (1970).
5. M. J. Stewart and F. Weinberg, Fluid flow through a solid–liquid dendritic interface, *Met. Trans.* **3,** 333–337 (1972).
6. S. Asai and I. Muchi, 1978, Theoretical analysis and model experiments on the formation mechanism of channel-type segregation, *Trans. ISIJ* **18,** 90–98 (1978).
7. J. Szekely and A. S. Jassal., An experimental and analytical study of the solidification of a binary dendritic system, *Met. Trans. B* **9,** 389–398 (1978).
8. M. E. Thompson and J. Szekely, Mathematical and physical modeling of double-diffusive convection of aqueous solutions crystallizing at a vertical wall, *J. Fluid Mech.* **187,** 409–433 (1988).
9. C. F. Chen, Onset of cellular convection in a salinity gradient due to a lateral temperature gradient, *J. Fluid Mech.* **63,** 563–576 (1974).
10. C. Beckermann, Melting and solidification and binary mixtures with double-diffusive convection in the melt, Ph.D. Thesis, Purdue University (1987).
11. M. A. Christenson and F. P. Incropera, Solidification of an aqueous ammonium chloride solution in a rectangular cavity—I. Experimental study, *Int. J. Heat Mass Transfer* **32,** 47–68 (1989).